Differential *M*-ary Orthogonal Signaling for DS/CDMA Land Mobile Satellite Communications

Athanassios C. Iossifides and Fotini-Niovi Pavlidou, *Member, IEEE*

***Abstract*— In this paper, we derive an analytical framework for the performance evaluation of a recently proposed *M*-ary orthogonal scheme based on differential encoding/decoding of the Walsh/Hadamard chips prior/after spreading. This technique makes feasible nonpilot-assisted detection over fast fading environments such as the land mobile satellite (LMS) channel. Our results show that differential *M*-ary orthogonal signaling presents very good performance at Doppler frequency shifts much higher than the symbol rate. Amplitude statistics are considered to be Rayleigh, but may be easily extended to more general models based on the analytical derivation presented.**

***Index Terms*— Doppler shift, DS/CDMA, fast fading, *M*-ary orthogonal modulation.**

I. Introduction

THE expanding demand for highly spectral efficient modulation techniques has well-established *M*-ary orthogonal signaling, by means of Walsh/Hadamard (W/H) sequences, for DS/CDMA applications. *M*-ary orthogonal DS/CDMA systems have already been applied or considered as strong candidates for terrestrial or future land mobile satellite (LMS) communications [1]–[5]. Although well suited for terrestrial applications, their effectiveness for LMS satellite systems is still under consideration, especially when nonpilot-aided demodulation is to be applied. This is mainly due to the special character of the LMS channel which originates crucial problems on the application of *M*-ary orthogonal signaling. One of the major problems is the tremendous performance degradation that *M*-ary orthogonal systems face under high Doppler frequency shifts [6], which are inherent in the LMS channel and may take values higher than the symbol rate [7]. This degradation results from loss of orthogonality of the transmitted waveforms, and makes conventional noncoherent detection impossible without any special device that removes Doppler shift. Such a device, together with a method of transmitting a combination of Hadamard sequences, was proposed in [7]. Instead of using a special device, and in order to keep complexity as low as possible, we have recently proposed two techniques based on chip-by-chip differential encoding before transmission [8]. This idea, based on [9], where chip-by-chip differential encoding of the spreading sequence was proposed for a BPSK DS/CDMA system, has driven us in a novel modulation/demodulation technique with differential encoding/decoding of W/H chips prior/after spreading, the so-called D*M*-ary orthogonal signaling. Preliminary simulation results presented in [8] under an LMS channel showed that the proposed scheme is capable of combating high Doppler shifts while preserving all the advantages of *M*-ary orthogonal modulation. In this paper, we concentrate on the analytical performance evaluation of a D*M*-ary orthogonal DS/CDMA system in order to find the range of applicability and the performance dynamics of the proposed scheme under a high Doppler shift environment. The analytical evaluation is applied at a Rayleigh fast fading environment, but generalization to more complex fading cases is straightforward as soon as the first- and second-order statistics of the fading process are known. The calculated results, in terms of the bit-error probability (BEP), are compared with the conventional envelope detected *M*-ary orthogonal scheme. Multiple-access interference is modeled as an extra additive Gaussian noise source [9]–[10], and nonperfect power control effects are not taken into account in order to focus on the signaling scheme.

The paper is organized as follows. In Section II, we describe the system model under consideration, including the transmitter, channel, and receiver models for both the differential and conventional *M*-ary orthogonal DS/CDMA systems. In Section III, we derive the BEP of the proposed scheme by first computing the pairwise error probability between two different Hadamard symbol/sequences. Computation of the conventional system's BEP is also included. In Section IV, we present comparative numerical results for both the differential and conventional systems under a Rayleigh fading environment, and we conclude our paper with Section V.

II. System Model

The transmitter of the conventional *M*-ary orthogonal system is shown in Fig. 1(a) while Fig. 1(b) presents the proposed D*M*-ary orthogonal DS/CDMA scheme (see also [8]). In both cases, b source information bits of rate r_b are grouped and mapped to one of $M = 2^b$ Hadamard symbols/sequences of rate $r_s = r_b/\log_2 M$. When no differential encoding is applied, the Hadamard chips $h_i^{(m)} \in \{\pm 1\}, 0 \le i, m \le M-1$ of period $T_H = T_s/M$, with T_s the symbol period, are oversampled by a factor $L = N/M$, which is assumed to be an integer, and then multiplied with a bipolar N-length random spreading sequence. The resulted samples BPSK modulate a T_c-energy chip waveform $\psi(t)$. The equivalent low-pass transmitted signal for the kth user in order to transmit the

Manuscript received March 6, 1998; revised June 8, 1998.

The authors are with the Department of Electrical and Computer Engineering, Telecommunications Division, School of Engineering, Aristotle University of Thessaloniki, 540 06 Thessaloniki, Greece.

Publisher Item Identifier S 0733-8716(99)01703-5.

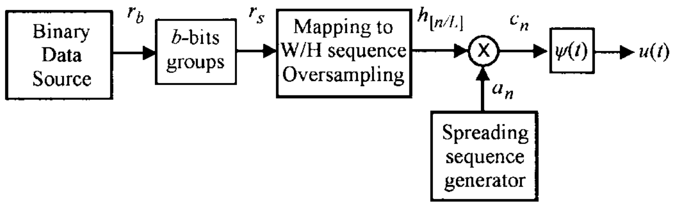

(a)

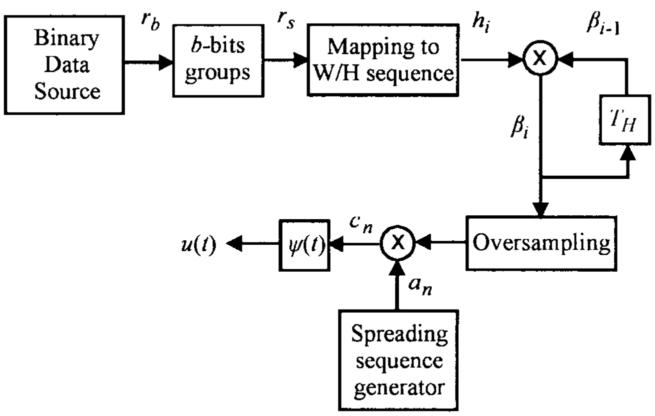

(b)

Fig. 1. Block diagrams of (a) DM-ary and (b) M-ary transmitters.

λth Hadamard symbol is

$$u^{(k)}(t) = \sqrt{2P} \sum_{n=0}^{N-1} c_n^{(k)} \psi(t - nT_c) \tag{1}$$

where

$$c_n^{(k)} = h_{\lfloor n/L \rfloor}^{(\lambda)} a_n^{(k)} \tag{2}$$

and $a_n^{(k)}$, $0 \le n \le N-1$ is the nth chip's amplitude of the characteristic for the kth user spreading sequence. P is the signal power.

When DM-ary orthogonal signaling is employed, the Hadamard chips are differentially encoded and then oversampled and spread, that is,

$$c_n^{(k)} = \beta_{\lfloor n/L \rfloor}^{(\lambda)} a_n^{(k)} \tag{3}$$

where $\beta_{\lfloor n/L \rfloor}^{(m)}$ are the oversampled differentially encoded Hadamard chips generated by

$$\beta_i^{(\lambda)} = \beta_{i-1}^{(\lambda)} h_i^{(\lambda)}. \tag{4}$$

The received low-pass signal takes the form

$$r(t) = g(t)u(t) + z(t) + J(t) \tag{5}$$

where $g(t)$ is a complex Gaussian random process representing the multiplicative fading process, $z(t)$ is the additive white Gaussian noise, and $J(t)$ is a random process representing multiple-access interference that results from interfering users. Assuming a perfect power control procedure and a large number of users, $J(t)$ may be approximated by a zero-mean Gaussian random process [9], [10]. Thus, we may introduce an equivalent white Gaussian noise process $n(t) = z(t) + J(t)$ for the combined effects of noise and multiple-access interference [9] with variance $N_0' = N_0 + J_0$, where N_0 and J_0 are power spectral densities of $z(t)$ and $J(t)$, respectively.

The receiver consists of a matched to the chip waveform filter with impulse response $\psi(-t)$, followed by a sampling (at the spreading chip rate) device. Perfect clock recovery and proper sampling instants are assumed so that interchip interference between the samples is eliminated (see also [9]). The complex-valued sequence that arises is multiplied with the locally generated spreading sequence, and enters an accumulator over the L spreading chips that are inherent in every Hadamard chip. The resulting samples during the interval of one Hadamard symbol take the form

$$r_i = \sqrt{2P} T_H g_i \beta_i^{(\lambda)} + n_i, \qquad 0 \le i \le M-1 \tag{6}$$

in case of the DM-ary orthogonal signaling and

$$r_i = \sqrt{2P} T_H g_i h_i^{(\lambda)} + n_i, \qquad 0 \le i \le M-1 \tag{7}$$

in the case of conventional M-ary orthogonal signaling. Assuming Rayleigh fading, the samples g_i of the multiplicative Gaussian fading process are complex, jointly Gaussian random variables. Their first and second moments are given by

$$E\{|g_i|^2\} = 1 \tag{8a}$$
$$E\{g_i\} = 0 \tag{8b}$$
$$\mathrm{var}(g_i) = 1/2 \tag{8c}$$
$$C(k) = \mathrm{cov}(g_i g_{i-k}^*) = \tfrac{1}{2} J_0(2\pi f_D T_H |k|) \tag{8d}$$

where f_D denotes the maximum Doppler shift. Introducing the normalized Doppler shift f_{DN}, so that $f_{DN} = f_D T_s$, the covariance may be written as $C(k) = \frac{1}{2} J_0(2\pi f_{DN} |k|/M)$. It should be noted that the above expressions are exact in the case of $L = 1$, that is, when one spreading chip is encountered for each Hadamard chip. When $L > 1$, the samples g_i of the channel in (6) and (7) arise after summation over L consecutive samples takes part. We assume that with proper normalization, the channel statistics are kept unaltered. Simulation results, to be presented, showed that the relationship between the length of the spreading sequence and M, that is, the number of spreading chips L per Hadamard chip, does not affect the performance under a constant level of multiple-access interference and noise N_0' as soon as the Doppler shift remains well below the Hadamard chip rate. Obviously, though, for longer spreading sequences leading to greater L, more users are needed to reach the same interference level. The noise samples n_i have variance $N_0' T_H$.

The analysis to be presented may be generalized to encounter more complex channel amplitude statistics, such as Rice (e.g., [11]), or combinations of Rice, Rayleigh, or log-normal statistics when the first and second statistical moments, as given by (8), are known.

The conventional receiver proceeds by passing the samples of (7) through a bank of M envelope correlators, one for each of the M Hadamard symbols/sequences [Fig. 2(a)]. The

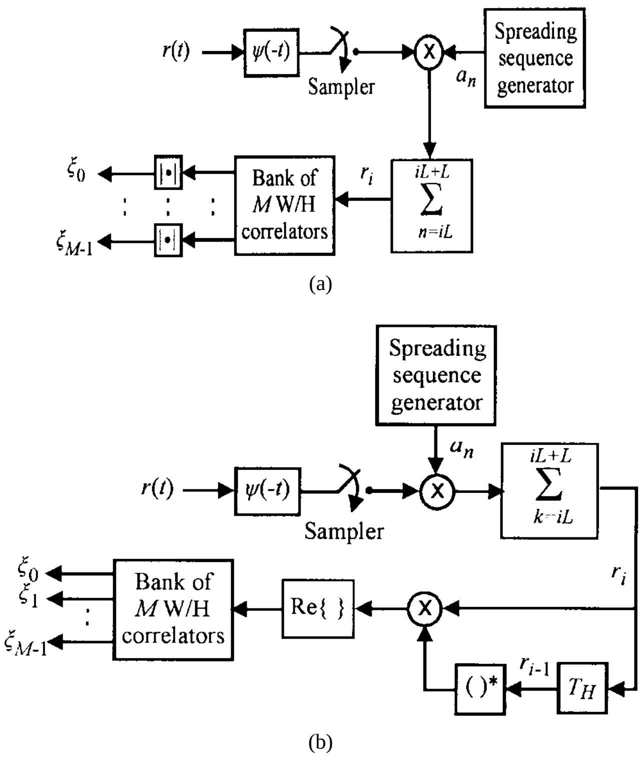

Fig. 2. Block diagrams of (a) D*M*-ary and (b) *M*-ary receivers.

decision variables that arise are

$$\xi_m = \left| \sum_{i=0}^{M-1} r_i h_i^{(m)} \right|, \qquad 0 \leq m \leq M-1. \tag{9}$$

The D*M*-ary receiver proceeds with differential decoding of the samples of (6), and then passes the decoded samples through the bank of correlators as shown in Fig. 2(b). The decision variables take the form

$$\xi_m = \sum_{i=0}^{M-1} \mathrm{Re}\{r_i r_{i-1}^*\} h_i^{(m)}, \qquad 0 \leq m \leq M-1. \tag{10}$$

In both cases, the symbol corresponding to the maximum decision variable is selected as the one transmitted. A symbol error occurs when $\xi_\lambda < \xi_m$, $0 \leq m \leq M-1$, $m \neq \lambda$, where λ was the transmitted symbol.

III. Error Probability Analysis

A. DM-ary Orthogonal Signaling

Let $P_{\lambda,m} = \Pr(\xi_\lambda - \xi_m < 0) = \Pr(D_{\lambda,m} < 0)$ denote the pairwise error probability (PEP) when symbol m is selected as correct over the transmitted symbol λ.

$$\begin{aligned} D_{\lambda,m} &= \sum_{i=0}^{M-1} \mathrm{Re}\{r_i r_{i-1}^*\} \delta_i^{(\lambda,m)} \\ &= \tfrac{1}{2} \sum_{i=0}^{M-1} (r_i^* r_{i-1} + r_i r_{i-1}^*) \delta_i^{(\lambda,m)} \end{aligned} \tag{11}$$

where $\delta_i^{(\lambda,m)} = h_i^{(\lambda)} - h_i^{(m)}$. Substituting the r_i's from (6), we get

$$\begin{aligned} D_{\lambda,m} = \tfrac{1}{2} \sum_{i=0}^{M-1} \Big[&\Big(\sqrt{2P} T_H g_i^* \beta_i^{(\lambda)} + n_i^*\Big) \\ &\times \Big(\sqrt{2P} T_H g_{i-1} \beta_{i-1}^{(\lambda)} + n_{i-1}\Big) \\ &+ \Big(\sqrt{2P} T_H g_i \beta_i^{(\lambda)} + n_i\Big) \\ &\times \Big(\sqrt{2P} T_H g_{i-1}^* \beta_{i-1}^{(\lambda)} + n_{i-1}^*\Big)\Big] \delta_i^{(\lambda,m)} \\ = \tfrac{1}{2} \sum_{i=0}^{M-1} \Big(&2PT_H^2 g_i^* g_{i-1} h_i^{(\lambda)} + \sqrt{2P} T_H \beta_i^{(\lambda)} g_i^* n_{i-1} \\ &+ \sqrt{2P} T_H \beta_{i-1}^{(\lambda)} g_{i-1} n_i^* + n_i^* n_{i-1} \\ &+ 2PT_H^2 g_i g_{i-1}^* h_i^{(\lambda)} + \sqrt{2P} T_H \beta_i^{(\lambda)} g_i n_{i-1}^* \\ &+ \sqrt{2P} T_H \beta_{i-1}^{(\lambda)} g_{i-1}^* n_i + n_i n_{i-1}^* \Big) \delta_i^{(\lambda,m)}. \end{aligned} \tag{12}$$

The sequence $(\delta^{(\lambda,m)})$ takes $M/2$ zero values and $M/2$ (± 2) values. The $M/2$ nonzero values are at these places where the elements of the two Hadamard sequences differ. Thus, different nonzero places, according to the specific symbols λ and m that are considered, arise. But, because of the structure of the Hadamard sequences, the same $(\delta^{(\lambda,m)})$ sequences (with different order) arise, no matter which symbol λ is taken as the reference symbol. Let $\boldsymbol{\Delta}_{\lambda,m}$ denote the set of i's corresponding to the $\delta_i^{(\lambda,m)}$ nonzero values regarding the symbols λ and m. The nonzero products $h_i^{(\lambda)} \delta_i^{(\lambda,m)}$, $i \in \boldsymbol{\Delta}_{\lambda,m}$ can be written as

$$h_i^{(\lambda)} \delta_i^{(\lambda,m)} = h_i^{(\lambda)} \Big(h_i^{(\lambda)} - h_i^{(m)} \Big) = 1 - h_i^{(\lambda)} h_i^{(m)}. \tag{13}$$

Since i refers to the nonzero positions of $(\delta^{(\lambda,m)})$, that is, the positions where the Hadamard sequences differ, the product $h_i^{(\lambda)} h_i^{(m)}$, $i \in \boldsymbol{\Delta}_{\lambda,m}$, always takes the value -1. Thus, $h_i^{(\lambda)} \delta_i^{(\lambda,m)} = 2$, for $i \in \boldsymbol{\Delta}_{\lambda,m}$. The products $\beta_i^{(\lambda)} \delta_i^{(\lambda,m)}$ and $\beta_{i-1}^{(\lambda)} \delta_i^{(\lambda,m)}$ may equal either $+2$ or -2. By absorbing the signs in the complex noise samples without changing their statistical properties, we can equivalently write (12) as

$$\begin{aligned} D_{\lambda,m} = \sum_{i \in \boldsymbol{\Delta}_{\lambda,m}} &2PT_H^2 g_i^* g_{i-1} + \sqrt{2P} T_H g_i^* n_{i-1} \\ &+ \sqrt{2P} T_H g_{i-1} n_i^* + n_i^* n_{i-1} \\ &+ 2PT_H^2 g_i g_{i-1}^* + \sqrt{2P} T_H g_i n_{i-1}^* \\ &+ \sqrt{2P} T_H g_{i-1}^* n_i + n_i n_{i-1}^*. \end{aligned} \tag{14}$$

Rearranging terms in (14) leads to

$$\begin{aligned} D_{\lambda,m} = \sum_{i \in \boldsymbol{\Delta}_{\lambda,m}} &\Big(\sqrt{2P} T_H g_i^* + n_i^*\Big)\Big(\sqrt{2P} T_H g_{i-1} + n_{i-1}\Big) \\ &+ \Big(\sqrt{2P} T_H g_i + n_i\Big)\Big(\sqrt{2P} T_H g_{i-1}^* + n_{i-1}^*\Big). \end{aligned} \tag{15}$$

Letting $y_i = \sqrt{2P} T_H g_i + n_i$, (15) may be rewritten as

$$D_{\lambda,m} = \sum_{i \in \boldsymbol{\Delta}_{\lambda,m}} y_i^* y_{i-1} + y_i y_{i-1}^*. \tag{16}$$

Since y_i are Gaussian random variables, (16) may be recognized as a Hermitian quadratic form of Gaussian random variables that can be written in matrix form as

$$D_{\lambda,m} = \boldsymbol{y}^\dagger \boldsymbol{F}_{\lambda,m} \boldsymbol{y} \tag{17}$$

where the superscript † denotes Hermitian transpose. The size of the vector $\boldsymbol{y}$ and the rectangular matrix $\boldsymbol{F}_{\lambda,m}$ vary with respect to the specific symbols λ and m, and may take values in the range $[M/2, M]$. Additionally, the specific samples y_i that take part in the quadratic form depend on λ and m. We dropped the superscripts λ, m from $\boldsymbol{y}$ for simplicity. The sets $\boldsymbol{\Delta}_{\lambda,m}$ together with the matrices $\boldsymbol{y}$ and $\boldsymbol{F}_{\lambda,m}$ that arise for $M = 8$ are given in detail in the Appendix. The PEP, that is, $P_{\lambda,m} = \Pr(D_{\lambda,m} < 0)$, can now be computed by evaluating the Laplace transform $\Phi_{D_{\lambda,m}}(s)$ of the probability density function of $D_{\lambda,m}$ and then using the inversion formula

$$P_{\lambda,m} = \frac{1}{2\pi j} \int_{c-j\infty}^{c+j\infty} \frac{1}{s} \Phi_{D_{\lambda,m}}(s)\, ds \tag{18}$$

with c chosen so that the integration path is contained in the intersection of the region of convergence of $\Phi_{D_{\lambda,m}}(s)$ and the right half-plane $\mathrm{Re}\, s > 0$ [11]. The Laplace transform of $D_{\lambda,m}$ is given by the general formula [12]

$$\Phi_{D_{\lambda,m}}(s) = \frac{\exp\left[-s\overline{\boldsymbol{y}}^\dagger \left(\boldsymbol{F}_{\lambda,m}^{-1} + 2s\boldsymbol{R}_{\lambda,m}^*\right)^{-1} \overline{\boldsymbol{y}}\right]}{\det(\boldsymbol{I} + 2s\boldsymbol{R}_{\lambda,m}^* \boldsymbol{F}_{\lambda,m})} \tag{19}$$

where $\overline{\boldsymbol{y}}$ is the mean of the vector $\boldsymbol{y}$, $\boldsymbol{R}_{\lambda,m}$ is the real-valued covariance matrix defined by $\boldsymbol{R}_{\lambda,m} = \frac{1}{2}E\{(\boldsymbol{y}-\overline{\boldsymbol{y}})^*(\boldsymbol{y}-\overline{\boldsymbol{y}})^T\}$, and $\boldsymbol{I}$ is the identity matrix of proper size. For the Rayleigh fading case under consideration, $E\{y_i\} = 0$, so $\overline{\boldsymbol{y}} = \boldsymbol{0}$. Thus, (19) can be simplified to

$$\Phi_{D_{\lambda,m}}(s) = \frac{1}{\det(\boldsymbol{I} + 2s\boldsymbol{R}_{\lambda,m}\boldsymbol{F}_{\lambda,m})} = \frac{1}{\prod\limits_i (1 + 2s\lambda_i)} \tag{20}$$

where λ_i are the eigenvalues of the product matrix $\boldsymbol{W}_{\lambda,m} = \boldsymbol{R}_{\lambda,m}\boldsymbol{F}_{\lambda,m}$. The elements of the covariance matrix $\boldsymbol{R}_{\lambda,m}$ can be easily computed by the second moments of $\boldsymbol{y}$, which after normalization with $2PT_H^2$, result in

$$\begin{aligned} \boldsymbol{R}_{\lambda,m} &\triangleq \{r_{i,j}\} = \frac{1}{2}E\{y_i y_j^*\} \\ &= \begin{cases} \frac{1}{2} + \frac{N_0'}{2PT_H} = \frac{1}{2} + \frac{MN_0'}{2\log_2 ME_b}, & i = j \\ \frac{1}{2}J_0(2\pi f_{DN}|i-j|/M), & i \neq j \end{cases} \end{aligned} \tag{21}$$

where the subscripts i, j take values governed by the set $\boldsymbol{\Delta}_{\lambda,m}$, specifically, the values of the set plus the new (not in the set already) values that come out by subtracting 1 from the set values. E_b is the signal energy per information bit. After substitution of (20) in (18), the PEP can be computed with several methods, such as saddle-point integration [9], [13], with the residues method [14] or with numerical integration by proper choice of the value of c as described in [11].

B. M-ary Orthogonal Signaling

The PEP of the conventional M-ary orthogonal scheme can be computed by observing that the decision variables ξ_m, $0 \le m \le M-1$ are Rayleigh distributed as the envelope of a Gaussian random variable that arises as a sum of Gaussian random variables. Therefore, the PEP $P_{\lambda,m} = \Pr(\xi_\lambda - \xi_m < 0)$ can be calculated with the formula [13]

$$P_{\lambda,m} = \int_0^\infty d\xi_\lambda \int_{\xi_\lambda}^\infty d\xi_m p(\xi_m, \xi_\lambda) \tag{22}$$

where $p(\xi_m, \xi_\lambda)$ is the joint probability density function of two Rayleigh random variables coming out as the envelope of two correlated Gaussian random processes, given by [12]

$$\begin{aligned} p(\xi_m, \xi_\lambda) = &\frac{\xi_m \xi_\lambda}{\sigma_m^2 \sigma_\lambda^2 (1-|\rho|^2)} I_0\left[\frac{|\rho|\xi_m\xi_\lambda}{\sigma_m\sigma_\lambda(1-|\rho|^2)}\right] \\ &\times \exp\left[-\frac{1}{2(1-|\rho|^2)}\left(\frac{\xi_\lambda^2}{\sigma_\lambda^2} + \frac{\xi_m^2}{\sigma_m^2}\right)\right], \\ &0 < \xi_m, \xi_\lambda \end{aligned} \tag{23}$$

where $2\sigma_\lambda^2 = E\{\xi_\lambda^2\}$, $2\sigma_m^2 = E\{\xi_m^2\}$, and ρ is the normalized complex cross covariance between the two complex Gaussian processes whose envelopes are represented by ξ_m, ξ_λ. Substituting for ξ_λ (9), we get

$$\begin{aligned} 2\sigma_\lambda^2 &= E\left\{\left(\sum_{i=0}^{M-1} r_i h_i^{(\lambda)}\right)\left(\sum_{j=0}^{M-1} r_j^* h_j^{(\lambda)}\right)\right\} \\ &= E\left\{\left(\sum_{i=0}^{M-1} \sqrt{2P}T_H g_i + n_i h_i^{(\lambda)}\right)\right. \\ &\qquad \left. \times \left(\sum_{j=0}^{M-1} \sqrt{2P}T_H g_j^* + n_i^* h_j^{(\lambda)}\right)\right\} \end{aligned} \tag{24}$$

where the product terms including a single noise sample or different noise samples have zero mean. Observing that there are M noise terms of the form $E\{n_i n_i^*\} = N_0 T_H$ and normalizing with $2PT_H^2$, we get

$$\begin{aligned} 2\sigma_\lambda^2 &= \frac{1}{2}\sum_{i=0}^{M-1}\sum_{j=0}^{M-1} J_0(2\pi f_{DN}|i-j|/M) + M\frac{N_0'}{2PT_H} \\ &= \frac{1}{2}\sum_{i=0}^{M-1}\sum_{j=0}^{M-1} J_0(2\pi f_{DN}|i-j|/M) + \frac{M^2 N_0'}{2\log_2 ME_b} \end{aligned} \tag{25}$$

since $PT_H = PT_s/M = \log_2 M \cdot PT_b/M = \log_2 M \cdot E_b/M$ with E_b the energy per transmitted bit. Similarly

$$\begin{aligned} 2\sigma_m^2 = &\frac{1}{2}\sum_{i=0}^{M-1}\sum_{j=0}^{M-1} h_i^{(\lambda)} h_i^{(m)} h_j^{(\lambda)} h_j^{(m)} J_0(2\pi f_{DN}|i-j|/M) \\ &+ \frac{M^2 N_0'}{2\log_2 ME_b}. \end{aligned} \tag{26}$$

The cross covariance may be written as

$$\begin{aligned}\rho &= \frac{1}{2\sigma_m\sigma_\lambda}E\left\{\left(\sum_{i=0}^{M-1} r_i h_i^{(\lambda)}\right)\left(\sum_{j=0}^{M-1} r_j^* h_j^{(m)}\right)\right\}\\ &= \frac{1}{2\sigma_m\sigma_\lambda}E\left\{\left(\sum_{i=0}^{M-1}\sqrt{2P}T_H g_i + n_i h_i^{(\lambda)}\right)\right.\\ &\qquad\left.\times\left(\sum_{j=0}^{M-1}\sqrt{2P}T_H g_j^* h_j^{(\lambda)} h_j^{(m)} + n_j^* h_j^{(m)}\right)\right\}.\end{aligned} \tag{27}$$

The difference in this case is that the pure noise terms result in a sum of the form $\Sigma_{i=1}^{M}\ E\{n_i n_i^*\}h_i^{(\lambda)}h_i^{(m)} = N_0' T_H\ \Sigma_{i=1}^{M}\ h_i^{(\lambda)}h_i^{(m)}$ which equals zero because of the orthogonality of the Hadamard sequences. Thus

$$\rho = \frac{1}{2\sigma_m\sigma_\lambda}\sum_{i=0}^{M-1}\sum_{j=0}^{M-1} h_j^{(\lambda)}h_j^{(m)}J_0(2\pi f_{DN}|i-j|/M). \tag{28}$$

It must be noted that, as in the case of D*M*-ary signaling, although the above parameters are different with respect to m leading in different PEP's, the same set of PEP's arises for every reference symbol λ.

The total symbol error probability, given that symbol λ was transmitted, may be upper bounded in both cases of *M*-ary and D*M*-ary signaling by the union of all of the error events, that is

$$P_{s|\lambda} \le \sum_{m=0, m\neq\lambda}^{M-1} P_{\lambda,m}. \tag{29}$$

Taking into account that all symbols are transmitted independently with equal probabilities and the set of PEP's is identical for every transmitted symbol, it is obvious that (29) accounts for the symbol error probability regardless of which was the transmitted symbol since $P_s = (1/M)\ \Sigma_{\lambda=0}^{M-1}\ P_{s|\lambda} = P_{s|\lambda}$. Finally, the BEP can be calculated as $P_b = P_s \cdot 2^{\log_2 M-1}/(2^{\log_2 M}-1)$.

IV. Results and Discussion

For the calculation of the PEP's in the D*M*-ary orthogonal case, we used either the method of residues or the method described in [11] when the number of eigenvalues is large. This second method is based on the reduction of the inverse Laplace integral of (18) in a sum using a Gauss–Chebyshev quadrature. The value of c was set equal to the one half of the real part of the pole of $\Phi_{D_{\lambda,m}}(s)$ with the smallest positive real part which corresponds (20) to the most negative eigenvalue (all eigenvalues are real).

In Fig. 3, we present simulation results of the BEP versus the signal to noise-plus-interference ratio E_b/N_0' for three different cases regarding the number of spreading chips L per Hadamard chip. The analytically derived BEP (union bound) is also shown for comparison purposes. Obviously, the value of L does not significantly change the performance of the system. Therefore, the assumption of $L = 1$ or that the channel statistics do not change when viewed at the Hadamard chip rate is valid. The independence of the BEP with respect to L is very important since the multiple-access interference reduction capability of the system is independent of the differential encoding process, in contrast to [9] where differential encoding was applied at the spreading chips.

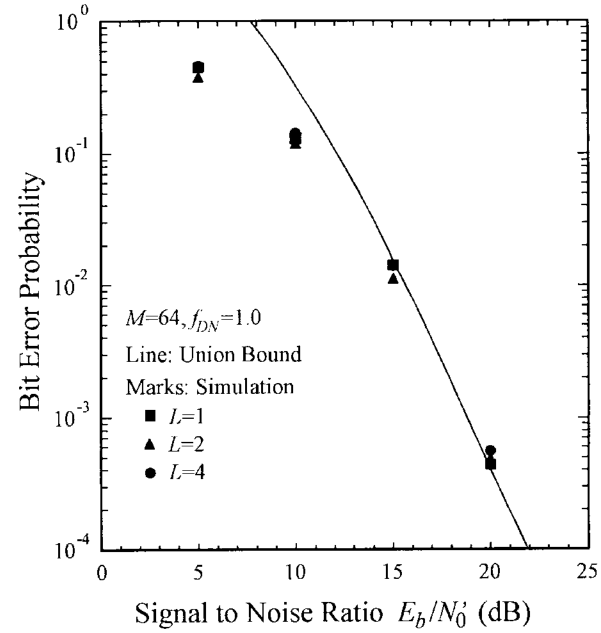

Fig. 3. D*M*-ary BEP simulation results for different numbers of spreading sequence chips per Hadamard chip in comparison with numerical BEP for $M = 64$ and normalized Doppler shift $f_{DN} = 1.0$.

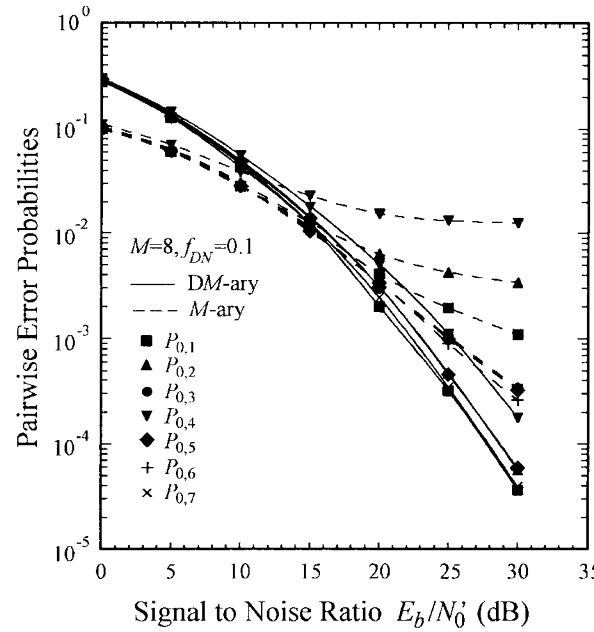

Fig. 4. PEP's of *M*-ary and D*M*-ary orthogonal signaling schemes for $M = 8$ at a normalized Doppler shift $f_{DN} = 0.1$.

Figs. 4 and 5 present the PEP's of the *M*-ary and D*M*-ary schemes at normalized Doppler shifts of 0.1 and 1.0, respectively, for $M = 8$. There are only five curves for the D*M*-ary scheme since, as explained in the Appendix, $P_{0,3} =$

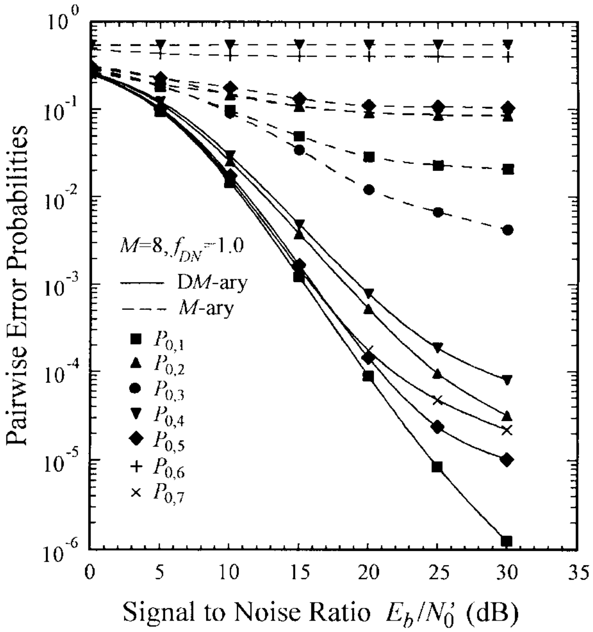

Fig. 5. PEP's of *M*-ary D*M*-ary orthogonal signaling schemes for $M = 8$ at a normalized Doppler shift $f_{DN} = 1.0$.

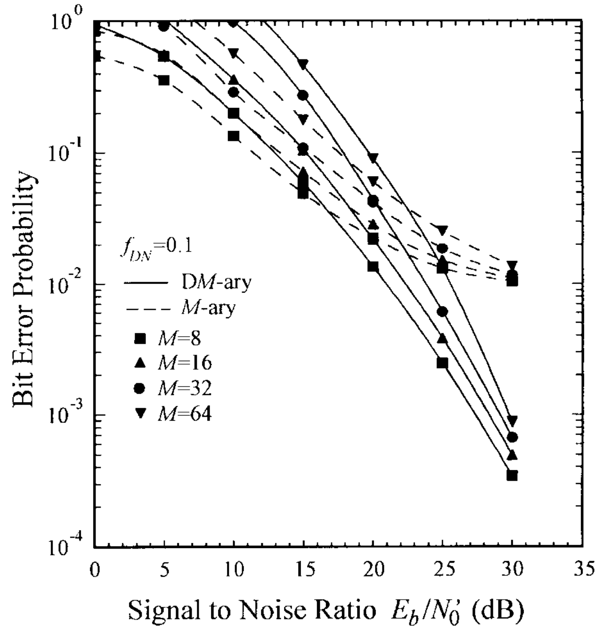

Fig. 6. BEP results of *M*-ary and D*M*-ary orthogonal signaling schemes at a normalized Doppler shift $f_{DN} = 0.1$ for various M.

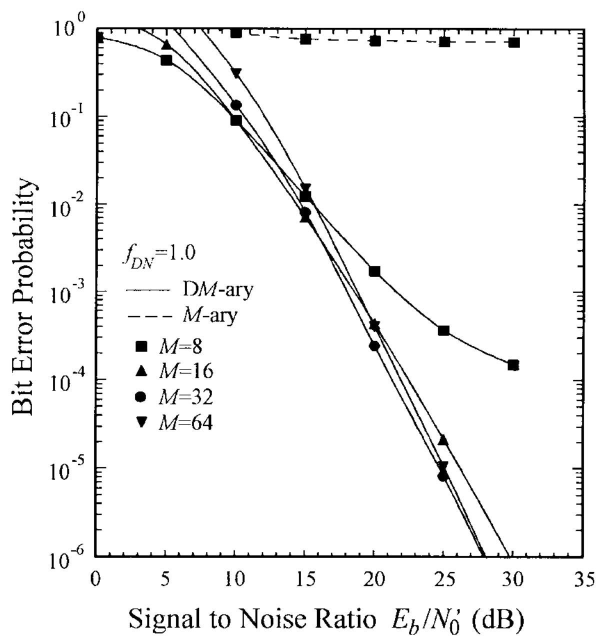

Fig. 7. BEP results of *M*-ary and D*M*-ary orthogonal signaling schemes at a normalized Doppler shift $f_{DN} = 1.0$ for various M.

$P_{0,2}$ and $P_{0,6} = P_{0,4}$. For low Doppler shift (Fig. 4), the conventional system's performance is better for low signal-to-noise ratios. This is expected because of the extra noncoherent combining loss introduced in the multiple differential decoding processes necessary for the detection of one symbol in the D*M*-ary case. But, for higher E_b/N_0', the PEP's of the *M*-ary case suffer from an error floor resulting from the Doppler shift. The performance enhancement of the D*M*-ary signaling is clear at higher Doppler shifts (Fig. 5). The resulting difference in the PEP's between the two schemes is several orders of magnitude. The total BEP is mainly governed, as can be easily deducted from (29) (see also [7]), by the worst PEP's. Therefore, the difference of the BEP's of the two schemes will be tremendous. It should also be noted that for $f_{DN} = 1.0$, an error floor occurs for D*M*-ary too, but at higher E_b/N_0'.

Figs. 6 and 7 show BEP results for the two schemes under consideration at normalized Doppler shifts of 0.1 and 1.0, respectively, for several symbol set sizes. For low Doppler shift (Fig. 6), the conventional scheme outperforms the differential scheme for signal to noise-plus-interference ratios under 15 dB due to the noncoherent combining loss mentioned above. For higher Doppler shifts (Fig. 7), the use of the conventional *M*-ary scheme is impossible since the orthogonality loss between the Hadamard symbols is crucial and leads to completely unacceptable performance in all cases of M. The $M = 8$ curve is only plotted for simplicity for the conventional case since curves for other M give almost the same result. On the other hand, D*M*-ary orthogonal signaling proves very resisting. The overall performance is enhanced as the Doppler shift takes higher values for all M cases. This behavior was also observed in [9], [15], and was explained as a "time diversity" effect since the faster signal distortions due to higher Doppler shift are averaged after correlation (that includes summation over the M samples) with the Hadamard sequences at the receiver. The error floor that the $M = 8$ case presents at $f_{DN} = 1.0$ will appear at higher Doppler shifts for larger symbol sets. This fact, together with the small performance difference between the several M values (increase of M leads to performance enhancement at $f_{DN} = 1.0$), guarantees better performance with larger symbol sets if we take into account the increase in bandwidth efficiency that greater M values offer. This, on the other hand, allows the use of longer spreading sequences as M increases, leading to multiple-access interference reduction and higher capacity.

In order to determine the range (with respect to Doppler shift) of applicability of D*M*-ary orthogonal signaling, we plot in Fig. 8 the BEP of both schemes versus the normalized

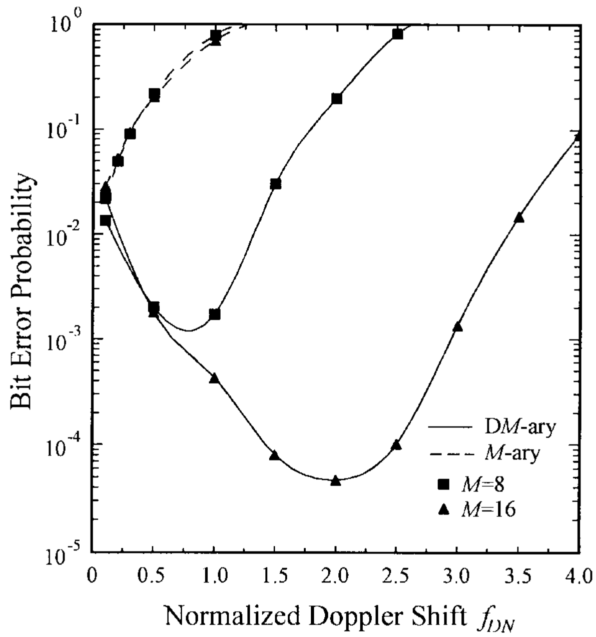

Fig. 8. BEP results of *M*-ary and D*M*-ary orthogonal signaling schemes versus the normalized Doppler shift for $M = 8$ and $M = 16$ at $E_b/N_0' = 20$ dB.

Doppler shift f_{DN}, for $M = 8$ and $M = 16$, at $E_b/N_0' = 20$ dB. Except from the clear performance enhancement that $M = 16$ offers with respect to $M = 8$, we observe that the lowest BEP occurs at a normalized Doppler shift on the order of $M/8$ (the minimum position with respect to f_{DN} does not change for other signal-to-noise ratios). Additionally, it is clear that an increase of M leads to a wider low-BEP region, which means that acceptable performance is evidenced in a wider range of Doppler shifts as M increases. For $M = 64$, the lower BEP will appear at $f_{DN} \simeq 8.0$. Assuming a symbol rate of $r_s = 2.67$ ksymbols/s ($r_b = 16$ kbits/s), the lower BEP will appear at a Doppler spread of about 21 kHz, which is normal to be evidenced in LMS channels. We, therefore, conclude that D*M*-ary signaling is well suited for LMS applications.

V. Conclusions

We presented and analyzed a differentially *M*-ary orthogonal (D*M*-ary) signaling scheme based on chip-by-chip differential encoding/decoding at the Hadamard chip level. Although we did not encounter a specific LMS channel model in our analysis, we presented a general analytical framework, and applied it to a Rayleigh fading environment characterized by high Doppler shifts that arise in LMS channels. The presented results showed that, while for low normalized Doppler shifts the conventional *M*-ary scheme performs better, the proposed scheme presents very good performance, and can effectively combat high Doppler shifts that appear in LMS channels, where conventional *M*-ary signaling is not applicable without any special device. It was shown that larger symbol sets lead to better performance, presenting minimum BEP at $f_{DN} \simeq M/8$. Therefore, D*M*-ary orthogonal signaling gives the opportunity of constructing bandwidth-efficient nonpilot-aided systems that combat high Doppler shift without any reduction of the multiple-access capability that maintains the well-known characteristics of *M*-ary orthogonal CDMA schemes.

Appendix

The quadratic forms that arise in the calculation of the PEP's consist of different size matrices regarding the symbols λ (reference symbol) and m that are encountered in the calculation of the PEP. As explained in Section III, the same $M-1$ sets $\boldsymbol{\Delta}_{\lambda,m}$ arise regardless of the reference symbol, thus producing identical quadratic forms. Here, the case of $M = 8$ is described in detail. The Hadamard matrix containing the eight possible transmitted sequences is

$$\boldsymbol{H} = \begin{bmatrix} 1 & 1 & 1 & 1 & 1 & 1 & 1 & 1 \\ 1 & -1 & 1 & -1 & 1 & -1 & 1 & -1 \\ 1 & 1 & -1 & -1 & 1 & 1 & -1 & -1 \\ 1 & -1 & -1 & 1 & 1 & -1 & -1 & 1 \\ 1 & 1 & 1 & 1 & -1 & -1 & -1 & -1 \\ 1 & -1 & 1 & -1 & -1 & 1 & -1 & 1 \\ 1 & 1 & -1 & -1 & -1 & -1 & 1 & 1 \\ 1 & -1 & -1 & 1 & -1 & 1 & 1 & -1 \end{bmatrix}. \quad (30)$$

Assuming, without loss of generality, that the reference symbol is the zeroth ($\lambda = 0$), the sets $\boldsymbol{\Delta}_{0,m}$, the vectors $\boldsymbol{y}$, and the matrices $\boldsymbol{F}_{0,m}$ that produce the quadratic forms for each one of the m symbols, $1 \le m \le M-1$ are

$$\boldsymbol{\Delta}_{0,1} = \{1,3,5,7\}, \quad \boldsymbol{y} = \begin{bmatrix} y_0 \\ y_1 \\ y_2 \\ y_3 \\ y_4 \\ y_5 \\ y_6 \\ y_7 \end{bmatrix},$$

$$\boldsymbol{F}_{0,1} = \begin{bmatrix} 0 & 1 & 0 & 0 & 0 & 0 & 0 & 0 \\ 1 & 0 & 0 & 0 & 0 & 0 & 0 & 0 \\ 0 & 0 & 0 & 1 & 0 & 0 & 0 & 0 \\ 0 & 0 & 1 & 0 & 0 & 0 & 0 & 0 \\ 0 & 0 & 0 & 0 & 0 & 1 & 0 & 0 \\ 0 & 0 & 0 & 0 & 1 & 0 & 0 & 0 \\ 0 & 0 & 0 & 0 & 0 & 0 & 0 & 1 \\ 0 & 0 & 0 & 0 & 0 & 0 & 1 & 0 \end{bmatrix}$$

$$\boldsymbol{\Delta}_{0,2} = \{2,3,6,7\}, \quad \boldsymbol{y} = \begin{bmatrix} y_1 \\ y_2 \\ y_3 \\ y_5 \\ y_6 \\ y_7 \end{bmatrix},$$

$$\boldsymbol{F}_{0,2} = \begin{bmatrix} 0 & 1 & 0 & 0 & 0 & 0 \\ 1 & 0 & 1 & 0 & 0 & 0 \\ 0 & 1 & 0 & 0 & 0 & 0 \\ 0 & 0 & 0 & 0 & 1 & 0 \\ 0 & 0 & 0 & 1 & 0 & 1 \\ 0 & 0 & 0 & 0 & 1 & 0 \end{bmatrix}$$

$$\boldsymbol{\Delta}_{0,3} = \{1,2,5,6\}, \quad \boldsymbol{y} = \begin{bmatrix} y_0 \\ y_1 \\ y_2 \\ y_4 \\ y_5 \\ y_6 \end{bmatrix},$$

$$\boldsymbol{F}_{0,3} = \begin{bmatrix} 0 & 1 & 0 & 0 & 0 & 0 \\ 1 & 0 & 1 & 0 & 0 & 0 \\ 0 & 1 & 0 & 0 & 0 & 0 \\ 0 & 0 & 0 & 0 & 1 & 0 \\ 0 & 0 & 0 & 1 & 0 & 1 \\ 0 & 0 & 0 & 0 & 1 & 0 \end{bmatrix}$$

$$\boldsymbol{\Delta}_{0,4} = \{4,5,6,7\}, \quad \boldsymbol{y} = \begin{bmatrix} y_3 \\ y_4 \\ y_5 \\ y_6 \\ y_7 \end{bmatrix},$$

$$\boldsymbol{F}_{0,4} = \begin{bmatrix} 0 & 1 & 0 & 0 & 0 \\ 1 & 0 & 1 & 0 & 0 \\ 0 & 1 & 0 & 1 & 0 \\ 0 & 0 & 1 & 0 & 1 \\ 0 & 0 & 0 & 1 & 0 \end{bmatrix}$$

$$\boldsymbol{\Delta}_{0,5} = \{1,3,4,6\}, \quad \boldsymbol{y} = \begin{bmatrix} y_0 \\ y_1 \\ y_2 \\ y_3 \\ y_4 \\ y_5 \\ y_6 \end{bmatrix},$$

$$\boldsymbol{F}_{0,5} = \begin{bmatrix} 0 & 1 & 0 & 0 & 0 & 0 & 0 \\ 1 & 0 & 0 & 0 & 0 & 0 & 0 \\ 0 & 0 & 0 & 1 & 0 & 0 & 0 \\ 0 & 0 & 1 & 0 & 1 & 0 & 0 \\ 0 & 0 & 0 & 1 & 0 & 0 & 0 \\ 0 & 0 & 0 & 0 & 0 & 0 & 1 \\ 0 & 0 & 0 & 0 & 0 & 1 & 0 \end{bmatrix}$$

$$\boldsymbol{\Delta}_{0,6} = \{2,3,4,5\}, \quad \boldsymbol{y} = \begin{bmatrix} y_1 \\ y_2 \\ y_3 \\ y_4 \\ y_5 \end{bmatrix},$$

$$\boldsymbol{F}_{0,6} = \begin{bmatrix} 0 & 1 & 0 & 0 & 0 \\ 1 & 0 & 1 & 0 & 0 \\ 0 & 1 & 0 & 1 & 0 \\ 0 & 0 & 1 & 0 & 1 \\ 0 & 0 & 0 & 1 & 0 \end{bmatrix}$$

$$\boldsymbol{\Delta}_{0,7} = \{1,2,4,7\}, \quad \boldsymbol{y} = \begin{bmatrix} y_0 \\ y_1 \\ y_2 \\ y_3 \\ y_4 \\ y_6 \\ y_7 \end{bmatrix},$$

$$\boldsymbol{F}_{0,7} = \begin{bmatrix} 0 & 1 & 0 & 0 & 0 & 0 & 0 \\ 1 & 0 & 1 & 0 & 0 & 0 & 0 \\ 0 & 1 & 0 & 0 & 0 & 0 & 0 \\ 0 & 0 & 0 & 0 & 1 & 0 & 0 \\ 0 & 0 & 0 & 1 & 0 & 0 & 0 \\ 0 & 0 & 0 & 0 & 0 & 0 & 1 \\ 0 & 0 & 0 & 0 & 0 & 1 & 0 \end{bmatrix}.$$

As shown, some of the arrays of quadratic forms are repeated, that is, $\boldsymbol{F}_{0,3} = \boldsymbol{F}_{0,2}$ and $\boldsymbol{F}_{0,6} = \boldsymbol{F}_{0,4}$. We also observe that the sets of the specific samples y_i that take part in the mentioned quadratic forms are a shifted version of each other, that is, the samples of the 0, 3 symbols' quadratic form can come out of the 0, 2 symbols' quadratic form by the transformation $y_i \to y_{i-1}$. This fact brings along equality of the corresponding covariance matrices, that is, $\boldsymbol{R}_{0,3} = \boldsymbol{R}_{0,2}$ and $P_{0,6} = P_{0,4}$, resulting in identical PEP's. It should also be noted that the product matrices $\boldsymbol{W}_{\lambda,m} = \boldsymbol{R}_{\lambda,m}\boldsymbol{F}_{\lambda,m}$, that are of the same size as $\boldsymbol{R}_{\lambda,m}$ and $\boldsymbol{F}_{\lambda,m}$, always have an even number of nonzero real eigenvalues, half of which are positive.

ACKNOWLEDGMENT

The authors are grateful to the anonymous reviewers for their helpful comments and suggestions.

REFERENCES

[1] M. Chase and K. Pahlavan, "Performance of DS/CDMA over measured indoor radio channels using random orthogonal codes," *IEEE Trans. Veh. Technol.*, vol. 42, pp. 617–621, Nov. 1993.

[2] L. F. Chang, F. Ling, D. D. Falconer, and N. R. Sollenberger, "Comparison of two convolutional orthogonal coding techniques for CDMA radio communications systems," *IEEE Trans. Commun.*, vol. 43, pp. 2028–2037, June 1995.

[3] A. C. Iossifides and F.-N. Pavlidou, "Performance of RS-coded DS/CDMA microcellular systems with *M*-ary orthogonal signaling," *Wireless Personal Commun.*, accepted for publication.

[4] A. Jalali and P. Melmenstein, "Effects of diversity, power control, and bandwidth on the capacity of microcellular CDMA systems," *IEEE J. Select. Areas Commun.*, vol. 12, pp. 952–961, June 1994.

[5] R. D. Gaudenzi, T. Garde, F. Gianneti, and M. Luise, "A performance comparison of orthogonal multiple access techniques for mobile satellite communications," *IEEE J. Select. Areas Commun.*, vol. 13, pp. 325–332, Feb. 1995.

[6] A. L. Kachelmyer and K. W. Forsythe, "*M*-ary orthogonal signaling in the presence of Doppler," *IEEE Trans. Commun.*, vol. 41, pp. 1192–1200, Aug. 1993.

[7] T. Wada, T. Yamazato, M. Katayama, and A. Ogawa, "A New *M*-ary/SSMA scheme applicable in LEO satellite communications systems," in *Proc. GLOBECOM'96*, London, England, Nov. 1996, pp. 384–389.

[8] A. C. Iossifides and F.-N. Pavlidou, "Performance of DS/CDMA systems with differential *M*-ary orthogonal modulation and RS-coding for LEO satellite communications," *Inter. Jour. on Satellite Commun*, accepted for publication.

[9] A. Cavallini, F. Giannetti, M. Luise, and R. Reggiannini, "Chip-level differential encoding/detection of spread-spectrum signals for CDMA radio transmission over fading channels," *IEEE Trans. Commun.*, vol. 45, pp. 456–463, Apr. 1997.

[10] A. J. Viterbi, *CDMA: Principles of Spread Spectrum Communication*. Reading, MA: Addison-Wesley, 1995.

[11] J. Ventura-Traveset, G. Caire, E. Biglieri, and G. Taricco, "Impact of diversity reception on fading channels with coded modulation—Part II: Differential block detection," *IEEE Trans. Commun.*, vol. 45, pp. 677–686, June 1997.

[12] M. Schwartz, W. R. Bennett, and S. Stein, *Communication Systems and Techniques*. New York: McGraw-Hill, Inc., 1966.

[13] C. W. Helstrom, *Elements of Signal Detection and Estimation*. Englewood Cliffs, NJ: Prentice-Hall, 1995.

[14] P. Ho and D. Fung, "Error performance of multiple-symbol differential detection of PSK signals transmitted over a correlated Rayleigh fading channels," *IEEE Trans. Commun.*, vol. 40, pp. 1566–1569, Oct. 1992.

[15] F. Giannetti, M. Luise, and R. Reggiannini, "Performance evaluation of a continuous-phase CDMA modem operating over the 60 GHz mobile radio channel," *Eur. Telecommun. Trans.*, vol. 7, pp. 255–265, May–June 1996.

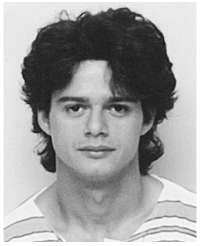

Athanassios C. Iossifides was born in Alexandroupolis, Greece, in 1969. He received the diploma in electrical engineering from Aristotle University of Thessaloniki, Greece, in 1994.

He is currently working toward the Ph.D. degree at Aristotle University of Thessaloniki. He is involved in European COST programs concerning mobile satellite or terrestrial communications, and he has served as a temporary Professor for the Technological Institute of Thessaloniki for two years. His main research interests lie in the area of terrestrial and satellite mobile communications, with emphasis on CDMA applications and channel coding techniques.

Mr. Iossifides is a member of the Technical Chamber of Greece.

Fotini-Niovi Pavlidou (S'86–M'87) received the Diploma in electrical and mechanical engineering and the Ph.D. degree in telecommunications networks from the Aristotle University of Thessaloniki, Greece, in 1979 and 1988, respectively.

She is with the Department of Electrical and Computer Engineering of the above Institution, where she offers courses on Mobile Communications and Telecommunications Networks. Her research interests include traffic analysis and design of networks, performance evaluation and QoS studies of mobile satellite communications, and multimedia applications over the Internet. She is involved in European Projects (Telematics, COST Actions, Tempus.), as well as in national projects in the referred scientific areas.

Dr. Pavlidou has served on the Program Committees (as a member or chairperson) of many conferences and workshops supported by IEEE/IEE. She is a member of the IEEE Communications Society and the Technical Chamber of Greece.